Ordinal Causal Discovery

Abstract

Causal discovery for purely observational, categorical data is a long-standing challenging problem. Unlike continuous data, the vast majority of existing methods for categorical data focus on inferring the Markov equivalence class only, which leaves the direction of some causal relationships undetermined. This paper proposes an identifiable ordinal causal discovery method that exploits the ordinal information contained in many real-world applications to uniquely identify the causal structure. The proposed method is applicable beyond ordinal data via data discretization. Through real-world and synthetic experiments, we demonstrate that the proposed ordinal causal discovery method combined with simple score-and-search algorithms has favorable and robust performance compared to state-of-the-art alternative methods in both ordinal categorical and non-categorical data. An accompanied R package `OCD` is freely available.

1 INTRODUCTION

Causal discovery [Spirtes et al., 2000, Pearl, 2009] is becoming increasingly more popular in machine learning, and finds numerous applications, e.g., biology [Sachs et al., 2005], psychology [Steyvers et al., 2003], and neuroscience [Shen et al., 2020], of which the prevailing goal is to discover causal relationships of variables of interest. The discovered causal relationships are useful for predicting a system's response to external interventions [Pearl, 2009], a key step towards understanding and engineering that system. While the gold standard for causal discovery remains the controlled experimentation, it can be too expensive, unethical, or even impossible in many cases, particularly on human beings. Therefore, inferring the unknown causal structures of complex systems from purely observational data is often desirable and, sometimes, the only option.

This paper considers causal discovery for ordinal categorical data. Categorical data are common across multiple disciplines. For example, psychologists often use questionnaires to measure latent traits such as personality and depression. The responses to those questionnaires are often categorical, say, with five levels (5-point Likert scale): "strongly disagree", "disagree", "neutral", "agree", and "strongly agree". In genetics, single-nucleotide polymorphisms are categorical variables with three levels (mutation on neither, one, or both alleles). Categorical data also arise as a result of discretization of non-categorical (e.g., continuous and count) data. For instance, in biology, gene expression data are often trichotomized to "underexpression", "normal expression", and "overexpression" [Parmigiani et al., 2002, Pe'er, 2005, Sachs et al., 2005] in order to reduce sequencing technical noise while retaining biological interpretability.

While causal discovery for purely observational categorical data have been extensively studied, the vast majority of existing methods [Heckerman et al., 1995, Chickering, 2002] have exclusively focused on Bayesian networks (BNs) with nominal (unordered) categorical variables. It has been well established that a nominal/multinomial BN is generally only identifiable up to *Markov equivalence class* in which all BNs encode the same Markov properties. For example, $X \to Y$ and $Y \to X$ are Markov equivalent and also distribution equivalent [Spirtes and Zhang, 2016] with a multinomial likelihood; therefore, they are non-identifiable with purely observational data.

In many real-world applications, categorical data (including the aforementioned Likert scale, single-nucleotide polymorphisms, and discretized gene expression data) contain ordinal information. In this paper, we show that this often-overlooked ordinal information is crucial in causal discovery for categorical data. We propose an ordinal causal discovery (OCD) method via an ordinal BN. Assuming causal Markov and causal sufficiency, we prove OCD to be identifiable in general for ordinal categorical data. Score-and-search

Submitted to the 38th Conference on Uncertainty in Artificial Intelligence (UAI 2022). **To be used for reviewing only**.

BN structure learning algorithms are developed – exhaustive search for small networks (e.g., bivariate data) and greedy search for moderate-sized networks. Through extensive experiments with real-world and synthetic datasets, we demonstrate that the proposed OCD is identifiable, robust, applicable to both categorical and non-categorical data, and competitive against a range of state-of-the-art causal discovery methods. To the best of our knowledge, we are the first to exploit the ordinal information for causal discovery in categorical data. Our major contributions are four-fold.

1. We advocate the usefulness of ordinal information of categorical data in causal discovery, which has been overlooked in the literature.
2. We propose the first causal discovery method, OCD, for ordinal categorical data.
3. We prove that OCD is generally identifiable for bivariate data, in contrast to the non-identifiability of multinomial BNs.
4. We demonstrate the strong utility of OCD by comparison with state-of-the-art alternatives using real-world and synthetic datasets.

1.1 RELATED WORK

For brevity, we review causal discovery methods that are fully identifiable with observational data.

Non-Categorical Data. Model-based BNs for continuous data are often represented as additive noise models. Under such representation, BNs are generally identifiable if the noises are non-Gaussian [Shimizu et al., 2006], if the functional form of the additive noise model is nonlinear [Hoyer et al., 2009, Zhang and Hyvärinen, 2009], or if the noise variances are equal [Peters and Bühlmann, 2014]. Also see much of the recent literature that focuses on bivariate causal discovery [Mooij et al., 2010, Janzing et al., 2012, Chen et al., 2014, Sgouritsa et al., 2015, Hernandez-Lobato et al., 2016, Marx and Vreeken, 2017, Blöbaum et al., 2018, Marx and Vreeken, 2019, Tagasovska et al., 2020]. For count data, Park and Raskutti 2015 proposed a Poisson BN and showed that it is identifiable based on the overdispersion property of Poisson BNs. By replacing overdispersion property with constant moments ratio property, Park and Park 2019 extended Poisson BNs to the generalized hypergeometric family which contains many count distributions such as binomial, Poisson, and negative binomial. Recently, Choi et al. 2020 developed a zero-inflated Poisson BN for zero-inflated count data.

Categorical Data. For nominal categorical data, causal identification, primarily focused on bivariate data, is possible under certain assumptions [Peters et al., 2010, Suzuki et al., 2014, Liu and Chan, 2016, Cai et al., 2018, Compton et al., 2020], e.g., when the categories admit hidden compact representations or when data follow a discrete additive noise model. However, to the best of our knowledge, causal discovery for ordinal data, which are very common in practice, has not been studied. Whether a categorical variable is ordinal or not is, in our opinion, easier to comprehend than the aforementioned assumptions of categorical data (e.g., discrete additive noise).

Mixed Data. There are recent developments for mixed data causal discovery [Cui et al., 2018, Tsagris et al., 2018, Sedgewick et al., 2019], some of which include categorical data. However, the ordinal nature of the categorical data is not exploited for causal identification; therefore, these algorithms output Markov equivalent BNs instead of individual BNs. The latent variable approach by Wei et al. [2018] could in principle be extended to ordinal data. However, the causal Markov assumption of latent variables cannot translate to the observed variables and the inferred causality does not have direct causal interpretation on the observed variables.

2 BIVARIATE ORDINAL CAUSAL DISCOVERY

We first introduce the proposed OCD method for bivariate data, which will be extended to multivariate data in Section 4. Let $(X, Y) \in \{1, \ldots, S\} \times \{1, \ldots, L\}$ denote a pair of ordinal variables with S and L levels, of which the possible causal relationships, $X \to Y$ or $Y \to X$, are under investigation. Throughout the paper, we make the causal Markov and causal sufficient assumptions, which are frequently adopted in the causal discovery literature [Pearl, 2009]. The former allows us to interpret the proposed model causally (beyond conditional independence) whereas the latter asserts that there are no unmeasured confounders.

The bivariate OCD considers the following probability distribution for causal model $X \to Y$,

$$p_{X \to Y}(X, Y) = p(X)p(Y|X), \tag{1}$$

where $p(X)$ is a multinomial/categorical distribution with probabilities $\boldsymbol{\pi} = (\pi_1, \ldots, \pi_S)$ with $\sum_{s=1}^{S} \pi_s = 1$, and $p(Y|X)$ is defined by an ordinal regression model [Agresti, 2003],

$$Pr(Y \leq \ell | X) = F(\gamma_\ell - \beta_X), \;\; \ell = 1, \ldots, L, \tag{2}$$

where β_X is a generic notation of $\beta_1, \ldots, \beta_S$ for $X = 1, \ldots, S$. Typical choices of the link function F are probit and inverse logit, which are empirically quite similar; hereafter we always use the probit link except for the identifiability theory, which is valid for both link functions. We fix $\gamma_1 = 0$ for ordinal regression parameter identifiability [Agresti, 2003]. Equation (2) implies the conditional probability distribution $Pr(Y = \ell | X = s) = F(\gamma_\ell - \beta_s) - F(\gamma_{\ell-1} - \beta_s)$ for $\ell = 1, \ldots, L$ and $s = 1, \ldots, S$ where $\gamma_0 = -\infty$ and $\gamma_L = \infty$. Let $\boldsymbol{\beta} = (\beta_1, \ldots, \beta_S)$ and $\boldsymbol{\gamma} = (\gamma_2, \ldots, \gamma_{L-1})$. We denote the model $p_{X \to Y}$ by

$p_{X\to Y}(X,Y|\boldsymbol{\pi},\boldsymbol{\beta},\boldsymbol{\gamma})$. Similarly, we define the probability model $p_{Y\to X}$ as $p_{Y\to X}(Y,X|\boldsymbol{\rho},\boldsymbol{\alpha},\boldsymbol{\eta})$. If the maximum likelihood estimate $\widehat{p}_{X\to Y}$ given observations of (X,Y) is strictly larger than $\widehat{p}_{Y\to X}$, then $X\to Y$ is deemed a more likely data generating causal model.

3 IDENTIFIABILITY

We will show that the proposed OCD is generally identifiable if at least one of the variable has at least three levels.

Definition 1 (Distribution Equivalence) *$p_{X\to Y}(X,Y|\boldsymbol{\pi},\boldsymbol{\beta},\boldsymbol{\gamma})$ and $p_{Y\to X}(Y,X|\boldsymbol{\rho},\boldsymbol{\alpha},\boldsymbol{\eta})$ are distribution equivalent if for any values of $(\boldsymbol{\pi},\boldsymbol{\beta},\boldsymbol{\gamma})$ there exist values of $(\boldsymbol{\rho},\boldsymbol{\alpha},\boldsymbol{\eta})$ such that $p_{X\to Y}(X,Y|\boldsymbol{\pi},\boldsymbol{\beta},\boldsymbol{\gamma}) = p_{Y\to X}(Y,X|\boldsymbol{\rho},\boldsymbol{\alpha},\boldsymbol{\eta})$ for any X,Y, and vice versa.*

Distribution equivalent causal models are clearly not distinguishable from each other by examining their observational distributions. The well-known multinomial BNs are distribution equivalent as illustrated in the following example.

Example 1 (Multinomial BN) *Consider a bivariate multinomial BN of $X\to Y$ whose conditional $p(Y|X)$ and marginal $p(X)$ probability distributions are given in Figure 1(a), and the joint distribution $p(X,Y)$ is given in Figure 1(b). Because of the multinomial assumption, we can find a set of parameters, i.e., the conditional $p(X|Y)$ and marginal $p(Y)$ probabilities (Figure 1(c)) of the reverse causal model $Y\to X$, which leads to the same joint distribution. Therefore, the probability distribution does not provide information for causal identification.*

Incorporating the underappreciated ordinal information, we will show that $p_{X\to Y}(X,Y|\boldsymbol{\pi},\boldsymbol{\beta},\boldsymbol{\gamma})$ and $p_{Y\to X}(Y,X|\boldsymbol{\rho},\boldsymbol{\alpha},\boldsymbol{\eta})$ are generally *not* distribution equivalent and are, therefore, identifiable.

Theorem 1 (Identifiability of OCD) *Let $X\in\{1,\dots,S\}$ and $Y\in\{1,\dots,L\}$ where $S,L\geq 2$ and $\max\{S,L\}\geq 3$. Suppose $X\to Y$ is the data generating causal model and the observational probability distribution of (X,Y) is given by*

$$p(X,Y) = p_{X\to Y}(X,Y|\boldsymbol{\pi},\boldsymbol{\beta},\boldsymbol{\gamma}).$$

For almost all $(\boldsymbol{\pi},\boldsymbol{\beta},\boldsymbol{\gamma})$ with respect to the Lebesgue measure, the distribution cannot be equivalently represented by the reverse causal model, i.e., there does not exist $(\boldsymbol{\rho},\boldsymbol{\alpha},\boldsymbol{\eta})$ such that,

$$p(X,Y) = p_{Y\to X}(Y,X|\boldsymbol{\rho},\boldsymbol{\alpha},\boldsymbol{\eta}), \forall X,Y.$$

The proof based on properties of real analytic functions is provided in the Supplementary Materials. We demonstrate Theorem 1 by revisiting Example 1.

Example 2 (Ordinal BN) *The conditional $p(Y|X)$ and marginal $p(X)$ probability distributions in Figure 1(a) coincide with those under the ordinal BN $p_{X\to Y}(X,Y|\boldsymbol{\pi},\boldsymbol{\beta},\boldsymbol{\gamma})$ with $\boldsymbol{\pi}=(0.25,0.25,0.5)$, $\gamma=1$, and $\boldsymbol{\beta}=(1,-1,1)$. Given a large enough dataset, the MLE of $p(X,Y)$ can be arbitrarily close to that in Figure 1(b). However, there does not exist any set of parameter values in the reverse causal model $p_{Y\to X}(Y,X|\boldsymbol{\rho},\boldsymbol{\alpha},\boldsymbol{\eta})$ that produces the conditional $p(X|Y)$ and marginal $p(Y)$ probability distributions in Figure 1(c). Therefore, the reverse causal model $p_{Y\to X}(Y,X|\boldsymbol{\rho},\boldsymbol{\alpha},\boldsymbol{\eta})$ cannot adequately fit the data generated from $p_{X\to Y}(X,Y|\boldsymbol{\pi},\boldsymbol{\beta},\boldsymbol{\gamma})$. For example, even with 100,000 observations, the MLE of $p(X,Y)$ under $p_{Y\to X}(Y,X|\boldsymbol{\rho},\boldsymbol{\alpha},\boldsymbol{\eta})$ still has a large bias (Figure 1(d)), which will never approach 0. Therefore, $p_{X\to Y}(X,Y|\boldsymbol{\pi},\boldsymbol{\beta},\boldsymbol{\gamma})$ can be distinguished from $p_{Y\to X}(Y,X|\boldsymbol{\rho},\boldsymbol{\alpha},\boldsymbol{\eta})$.*

Note that Theorem 1 excludes the case where both X and Y are binary (i.e., $L=S=2$), under which OCD is not identifiable. This is expected because there is no difference between ordinal and nominal categorical variables in this case; the latter is known to be non-identifiable.

4 EXTENSION TO MULTIVARIATE ORDINAL CAUSAL DISCOVERY

While the vast majority of the existing identifiable causal discovery methods for categorical data [Peters et al., 2010, Suzuki et al., 2014, Liu and Chan, 2016, Cai et al., 2018, Compton et al., 2020] have primarily focused on bivariate cases, we extend the proposed bivariate OCD to multivariate data. Let $\boldsymbol{X}=(X_1,\dots,X_p)\in\{1,\dots,L_1\}\times\cdots\times\{1,\dots,L_p\}$ denote p ordinal variables. Let $G=(V,E)$ denote a causal BN with a set of nodes $V=\{1,\dots,p\}$ representing $\boldsymbol{X}$ and directed edges $E\subset V\times V$ representing direct causal relationships (with respect to $\boldsymbol{X}$). Let $pa(j)=\{k|k\to j\}\subseteq V$ denote the set of direct causes (*parents*) of node j in G and let $\boldsymbol{X}_{pa(j)}=\{X_k|k\in pa(j)\}$. Given G, the joint distribution of $\boldsymbol{X}$ factorizes,

$$p(\boldsymbol{X}|G)=\prod_{j=1}^{p} p\left(X_j|\boldsymbol{X}_{pa(j)}\right), \tag{3}$$

where each conditional distribution $p\left(X_j|\boldsymbol{X}_{pa(j)}\right)$ is an ordinal regression model of which the cumulative distribution is given by, for $\ell=1,\dots,L_j$,

$$Pr(X_j\leq\ell|\boldsymbol{X}_{pa(j)})=F\left(\gamma_{j\ell}-\sum_{k\in pa(j)}\beta_{jkX_k}-\alpha_j\right),$$

where α_j is the intercept and β_{jkX_k} is a generic notation of $\beta_{jk1},\dots,\beta_{jkL_k}$ for $X_k=1,\dots,L_k$. We set

$P(Y\|X)$	$X=1$	$X=2$	$X=3$
$Y=1$	0.16	0.84	0.16
$Y=2$	0.34	0.14	0.34
$Y=3$	0.50	0.02	0.50

(a)

$\times$

X	$P(X)$
1	0.25
2	0.25
3	0.50

$P(X,Y)$	$X=1$	$X=2$	$X=3$
$Y=1$	0.040	0.210	0.080
$Y=2$	0.085	0.035	0.170
$Y=3$	0.125	0.005	0.250

(b)

$P(X\|Y)$	$Y=1$	$Y=2$	$Y=3$
$X=1$	0.12	0.29	0.33
$X=2$	0.64	0.12	0.01
$X=3$	0.24	0.59	0.66

(c)

$\times$

Y	$P(Y)$
1	0.33
2	0.29
3	0.38

$\hat{P}(X,Y)$	$X=1$	$X=2$	$X=3$
$Y=1$	0.104	0.087	0.141
$Y=2$	0.065	0.071	0.154
$Y=3$	0.078	0.089	0.211

(d)

Figure 1: Illustration. (a) Conditional $p(Y|X)$ and marginal $p(X)$ probability distributions. They coincide with those under $p_{X\to Y}(X,Y|\boldsymbol{\pi},\boldsymbol{\beta},\boldsymbol{\gamma})$ with $\boldsymbol{\pi}=(0.25,0.25,0.5)$, $\gamma=1$, and $\boldsymbol{\beta}=(1,-1,1)$. (b) The joint distribution $p(X,Y)=p(X)p(Y|X)$. (c) Conditional $p(X|Y)$ and marginal $p(Y)$ probability distributions from the same joint distribution $p(X,Y)$. (d) Maximum likelihood estimate of $p(X,Y)$ under $p_{Y\to X}(Y,X|\boldsymbol{\rho},\boldsymbol{\alpha},\boldsymbol{\eta})$ using data generated from $p(X,Y)$ in (b) with sample size 100,000.

$\gamma_{j1}=\beta_{jkL_k}=0$ for ordinal regression parameter identifiability [Agresti, 2003]. The implied conditional probability distribution $Pr(X_j=\ell|\boldsymbol{X}_{pa(j)}=\boldsymbol{s})=F(\gamma_{j\ell}-\sum_{k\in pa(j)}\beta_{jkh_k}-\alpha_j)-F(\gamma_{j,\ell-1}-\sum_{k\in pa(j)}\beta_{jkh_k}-\alpha_j)$ for $\ell=1,\ldots,L_j$ and $\boldsymbol{s}\in\prod_{k\in pa(j)}\{1,\ldots,L_k\}$. In summary, the multivariate OCD model is parameterized by $\boldsymbol{\gamma}_j=(\gamma_{j2},\ldots,\gamma_{j,L_j-1})$, $\boldsymbol{\beta}_{jk}=(\beta_{jk1},\ldots,\beta_{jk,L_k-1})$, and α_j, for $j=1,\ldots,p$ and $k\in pa(j)$.

5 CAUSAL GRAPH STRUCTURE LEARNING

We develop simple score-and-search learning algorithms to estimate the structure of causal graphs, which already show strong empirical performance (see Section 6), although more sophisticated learning methods such as Bayesian inference could be adopted to further improve the performance.

Score. We score causal graphs by the Bayesian information criterion (BIC). We choose BIC over AIC because it favors a more parsimonious causal graph due to the heavier penalty on model complexity and generally has a better empirical performance. Let $\boldsymbol{x}=(\boldsymbol{x}_1,\ldots,\boldsymbol{x}_n)$ denote n realizations of $\boldsymbol{X}$. The score of G (smaller is better) is given by

$$\text{BIC}(G|\boldsymbol{x})=-2\sum_{i=1}^{n}\log\widehat{p}(\boldsymbol{x}_i|G)+K\log(n),$$

where K is the number of model parameters and $\widehat{p}(\boldsymbol{x}_i|G)$ is the joint distribution (3) evaluated at $\boldsymbol{x}_i$ given the MLE of model parameters.

Exhaustive Search. For small networks (say $p=2$ or 3), we compute the scores for all networks $\mathcal{G}$, and identify $\widehat{G}=\arg\min_{G\in\mathcal{G}}\text{BIC}(G|\boldsymbol{x})$. While this approach is exact and useful for bivariate OCD, it becomes computationally infeasible for moderate-sized networks as the number of networks $|\mathcal{G}|$ grows super-exponentially in p.

Greedy Search. We use a simple iterative greedy search algorithm [Chickering, 2002, Scutari et al., 2019] for moderate-sized networks. At each iteration, we score all the graphs that can be reached from the current graph by an edge addition, removal, or reversal. We replace the current graph by the graph with the largest improvement (largest decrease in BIC) and stop the algorithm when the score can no longer be improved. The greedy search algorithm is summarized in Algorithm 1 which is guaranteed to find a local optimal graph. The algorithm can be improved by tabu search and random non-local moves [Scutari et al., 2019] but we do not pursue this direction as the simple greedy algorithm already yields favorable results against state-of-the-art alternative methods. The worst per iteration cost is $O(pf(n,m,L))$ for p nodes, n observations, m maximum number of parents, and $L=\max_j L_j$ maximum levels, where $f(n,m,L)$ is the computational complexity of an ordinal regression with m regressors. This is because at most $2p$ score evaluations are required at each iteration [Scutari et al., 2019]. We use `polr` function in the R package `MASS` for ordinal regression which appears to scale linearly in n,m, and L, empirically.

6 EXPERIMENTS

We evaluate the proposed and state-of-the-art alternative causal discovery methods with synthetic as well as three sets of real data. The real data are not categorical and therefore allow us to extend our comparison to causal models designed for continuous data.

Algorithm 1 Greedy Search

Input: data $\boldsymbol{x}$, initial graph G
Compute BIC($G|\boldsymbol{x}$) and set BIC$_\star$=BIC($G|\boldsymbol{x}$).
repeat
  Initialize $Improvement = false$.
  for all graphs G' reachable from G **do**
    Compute BIC($G'|\boldsymbol{x}$).
    if BIC($G'|\boldsymbol{x}$) $<$ BIC$_\star$ **then**
      Set $G = G'$ and BIC$_\star$=BIC($G'|\boldsymbol{x}$)
      Set $Improvement = true$.
    end if
  end for
until $Improvement$ is $false$
Output: graph G

6.1 SYNTHETIC ORDINAL DATA

We simulate low-dimensional, higher-dimensional, and bivariate (with confounders) synthetic ordinal data.

6.1.1 Low-Dimensional Multivariate Ordinal Data

We consider synthetic ordinal data ($n = 500, p = 10$). To mimic survey data with 5-point Likert-scale questionnaires, we simulate data from the proposed OCD model with $L_j = L = 5, \forall j$. The true BN is generated randomly (Figure 2(a)) which has one v-structure (i.e., subgraph $j \to k \leftarrow i$). Its Markov equivalence class, represented by a completed partially directed acyclic graph (CPDAG), can be obtained by removing the directionality of the red dashed edges in Figure 2(a). We consider 6 scenarios with different levels of signal strength by generating simulation true $\beta_{jk\ell}$'s and α_j's independently from $N(0, \sigma^2)$ with $\sigma = 0.25, 0.5, 0.75, 1, 1.25, 1.5$. Parameters $\gamma_{j\ell}$'s are chosen to have balanced class size for each variable.

Implementations. Standard causal discovery methods for categorical data are multinomial BNs with BIC or BDe score which discard the ordinal information and therefore only estimate the Markov equivalence classes. They are implemented using model averaging with 500 bootstrapped samples (page 145, Scutari and Denis 2014). We compare them with the proposed OCD, all implemented using greedy search. In addition, we also consider a two-step procedure [Friedman and Koller, 2003] which first learns a causal ordering and then estimates the causal multinomial BN given the ordering based on BIC (called "BIC+" hereafter). This procedure outputs an estimated BN.

Metrics. We compute the structural hamming distance (SHD) and the structural intervention distance (SID) with R package `SID`. The SHD between two graphs is the number of edge additions, deletions, or reversals required to transform one graph to the other. The SID measures "closeness" between two causal graphs in terms of their implied intervention distributions (see Peters and Bühlmann 2015 for the formal definition). Note that since multinomial BNs with BIC and BDe can only identify CPDAG, the smallest SHD that they can achieve is 5 (the number of undirected edges in the true CPDAG).

Results. The SHD and SID averaged over 5 repeat simulations are shown in Figure 2(b)-(c) as functions of signal strength σ. Since multinomial BNs with BDe and BIC only estimate CPDAGs, we report the lower bounds of their SID. There are several conclusions that can be drawn. First, OCD is empirically identifiable because both SHD and SID quickly approach 0 as signal becomes stronger. Second, OCD uniformly outperforms the alternative methods in both SHD and SID across all signal levels, which suggests that exploiting the ordinal nature of ordinal categorical data is crucial for causal discovery. Third, BIC+ is better than BIC and BDe in SHD but not necessarily in SID, suggesting the estimated causal ordering from BIC+ is biased.

Different Number of Categories. In the Supplementary Materials, we present additional simulation scenarios with a different number $L = 3$ of categories. Similarly to the scenarios with $L = 5$, OCD significantly outperforms the competing methods.

6.1.2 Higher-Dimensional Multivariate Ordinal Data

We fix the sample size $n = 500$ and the number of categories $L = 5$ but vary the number of nodes $p = 10, 20, \ldots, 100$ and the signal strength $\sigma = 0.25, 0.5, 0.75, 1$. The graphs are kept at the same sparsity as in Section 6.1.1 across p (denser graphs will be considered later). The SHD is shown in Figure 3 whereas the SID is provided in the Supplementary Materials due to the space limit. The proposed OCD uniformly outperforms the competing methods BDe, BIC, and BIC+ across p and σ. In general, OCD is quite stable as p increases when the signal strength is moderate to moderately large $\sigma \geq 0.5$ whereas the competing methods quickly deteriorate with p regardless of the signal strength.

Scalability. We investigate the scalability of the proposed OCD with respect to n, L, and p. We vary $n = 500, 750, \cdots, 2750$ (keeping $p = 10$ and $L = 5$), $L = 5, \ldots, 14$ (keeping $n = 500$ and $p = 10$), and $p = 10, 20, \ldots, 100$ (keeping $n = 500$ and $L = 5$). The total CPU times in seconds on a 2.9 GHz 6-Core Intel Core i9 laptop are provided in the Supplementary Materials. The greedy search appears to scale linearly in n and L, and quadratically in p, which agrees with the complexity analysis in Section 5. It is moderately scalable: e.g., for $p = 100$, the search completes in about 3 hours.

Denser Graphs. In the Supplementary Materials, we present additional simulation scenarios with denser graphs for $p = 50$ nodes and more v-structures, which lead to similar conclusions, i.e., OCD significantly outperforms the

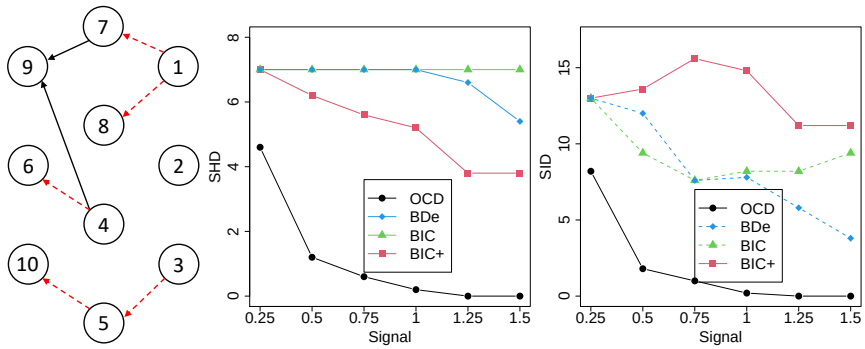

(a) True DAG (b) SHD (c) SID

Figure 2: Synthetic ordinal data. The dashed lines in (c) are the lower bounds of SID of BDe and BIC which output CPDAGs instead of BNs.

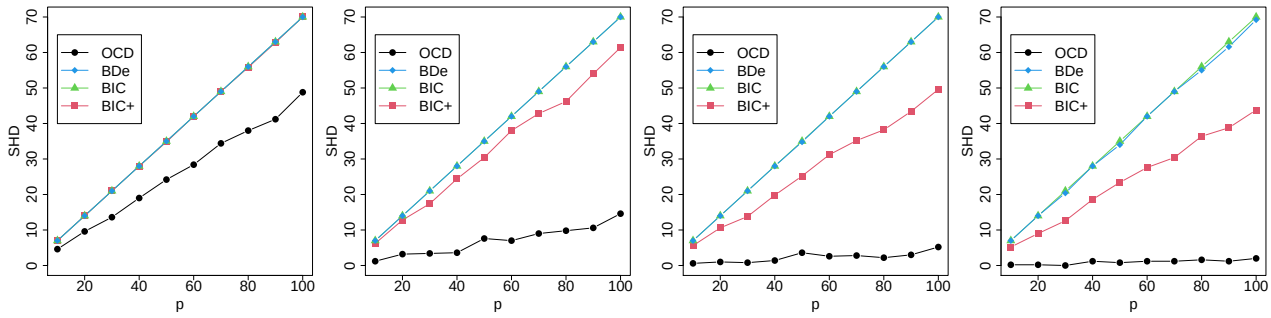

(a) SHD in p ($\sigma = 0.25$) (b) SHD in p ($\sigma = 0.5$) (c) SHD in p ($\sigma = 0.75$) (d) SHD in p ($\sigma = 1$)

Figure 3: SHD for OCD, BDe, BIC, and BIC+ as functions of p in the synthetic ordinal data with the sample size fixed at $n = 500$ and different signal strength $\sigma \in \{0.25, 0.5, 0.75, 1\}$.

competing methods in SHD and SID.

6.1.3 Bivariate Ordinal Data with Unmeasured Confounders

While our identifiability theory assumes no unmeasured confounders, we now empirically test the sensitivity of OCD to unmeasured confounders for bivariate ordinal data. We generate trivariate ordinal data (X_1, X_2, X_3) with $L = 5$ from the following true causal graph,

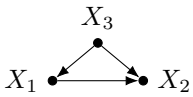

We hide X_3 as a confounder and apply OCD to (X_1, X_2). In the simulation truth, we assume $\beta_{jk\ell}$, for each $\ell = 1, \ldots, L$, to be the same for all $j \neq k$, i.e., the confounding effect is the same as the causal effect, which is simulated from $N(0, \sigma^2)$. We consider different levels of signal strength $\sigma = 0.25, 0.5, 0.75, 1, 1.25, 1.5$ and different sample sizes $n = 100, 200, \ldots, 1000$. Under each combination of (σ, n), we repeat the experiment 100 times, and report the average accuracy (ACC) for *forced decisions*. The forced decision forces methods to choose between $X_1 \to X_2$ and $X_2 \to X_1$. The same metric has been used in similar bivariate causal discovery problems [Mooij et al., 2016, Tagasovska et al., 2020]. OCD is relatively robust to confounders (Figure 4(a)): it is able to correctly identify the causal direction given a large enough sample size or when the signal is sufficiently strong. For comparison, we apply a recent causal discovery method for bivariate nominal categorical data, HCR [Cai et al., 2018]. Its average ACC is shown in Figure 4(b). We find the ACC of HCR is uniformly lower than that of OCD although we note that HCR is not specifically designed for this task.

6.2 SACHS'S SINGLE-CELL FLOW CYTOMETRY DATA

We evaluate the proposed OCD on the well-known single-cell flow cytometry dataset [Sachs et al., 2005], which contains measurements of 11 phosphorylated proteins under different experimental conditions. Sachs et al. 2005 provided a consensus causal network of these proteins, which could be used to gauge the performance of causal discovery

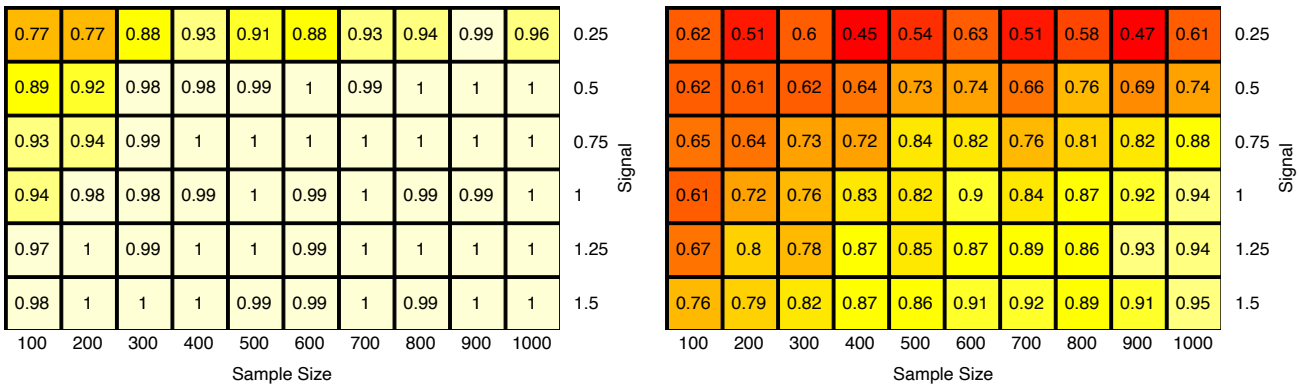

(a) Average ACC of OCD

(b) Average ACC of HCR

Figure 4: Synthetic ordinal data with confounders. Average ACC of (a) OCD and (b) HCR under different sample sizes and levels of signal strength.

algorithms. As in Tagasovska et al. 2020, we consider the *cd3cd28* dataset with 853 cells subject to the same experimental condition.

Implementations. Since the raw measurements are highly skewed and heavy-tailed, Sachs et al. 2005 discretized the data into $L = 3$ levels ("low", "average", and "high") and fit a multinomial BN based on the Bayesian Dirichlet equivalent uniform (BDe) score [Heckerman et al., 1995]. As we will see, this approach throws away the ordinal information inherent in the raw measurements and hence significantly underperforms OCD (with greedy search). For comparison, we also apply ANM [Hoyer et al., 2009], LiNGAM [Shimizu et al., 2006], RESIT with the Gaussian process implementation [Peters et al., 2014], bivariate causal discovery methods (HCR, bQCD [Tagasovska et al., 2020], GR-AN [Hernandez-Lobato et al., 2016], IGCI with uniform measure [Janzing et al., 2012], SLOPE [Marx and Vreeken, 2017]), and methods inferring Markov equivalence classes (PC [Spirtes et al., 2000], CPC [Ramsey et al., 2012], GES [Chickering, 2002], IAMB [Tsamardinos et al., 2003], multinomial BNs with BIC and BDe), and the mixed data approach MXM [Tsagris et al., 2018] to the raw continuous data. For bivariate causal discovery methods, we follow a similar *ad hoc* procedure in Tagasovska et al. 2020: first run CAM [Bühlmann et al., 2014] and then orient the estimated edges by the bivariate methods. HCR is the closest competitor as it is also designed for categorical data although with a very different scope (only applicable to bivariate nominal categorical data and assuming the existence of hidden compact representations).

Metrics. We use the same SHD and SID metrics as in Section 6.1. For methods that output CPDAGs instead of BNs, we report the lower and upper bounds of SID.

Results. In Table 1, we summarize the SHD and SID. OCD shows very strong performance comparing to state-of-the-art alternatives. It has the lowest SHD and the second lowest SID, which shows benefit of discretization for highly noisy data. The substantial improvement of OCD from multinomial BN with BDe (SHD 14 vs 21) highlights the importance of exploiting the ordinal information of discrete data for causal discovery. While there is strong motivation (e.g., biological interpretation) to use $L = 3$ for this dataset, we test OCD with L up to 10. OCD stays very competitive within this range: the SID remains 62 for all L whereas the SHD slightly increases as L increases possibly due to relatively small sample size, e.g., SHD $= 16$ for $L = 10$, which is still quite competitive (second to SHD $= 15$ for bQCD and IGCI).

Table 1: Sachs's data. Methods (marked by *) that are only applicable to bivariate data are combined with CAM. PC, CPC, GES, IAMB, BIC, BDe, and MXM only learn CPDAGs; we provide the lower and upper bounds of SID.

	OCD	bQCD*	IGCI*	GR-AN*
SHD	14	15	15	16
SID	62	69	82	80
	HCR*	SLOPE*	ANM	LiNGAM
SHD	16	17	17	17
SID	76	86	78	86
	PC	CPC	GES	IAMB
SHD	18	18	18	20
SID	50-83	50-80	50-80	79-70
	BIC	BDe	MXM	RESIT
SHD	20	21	21	40
SID	53-77	49-104	49-104	45

6.3 CAUSEEFFECTPAIRS (CEP) BENCHMARK DATA

We consider the CauseEffectPairs (CEP) benchmark data [Mooij et al., 2016] (version: 12/20/2017), which contain 108 datasets from 37 domains (e.g., biology, economy, engi-

neering, and meteorology). Each dataset contains a pair of variables (X, Y) for which the causal relationship is clear from the context, e.g., older "age" causes higher "glucose". We retain the same 99 pairs as in Tagasovska et al. 2020 that have univariate non-binary cause and effect variables.

Implementations. We compare OCD with HCR, bQCD, IGCI, CAM, SLOPE, LiNGAM, and RESIT. To apply OCD and HCR, we discretize each variable at $L - 1$ quantiles for $L \in \{10, \ldots, 20\}$. All other methods are applied to the (standardized) continuous data without discretization.

Metrics. We compute the ACC for forced decisions as in Section 6.1.3 and, additionally, the *area under the receiver operating curve* (AUC) for *ranked decision*. The ranked decision ranks the confidence of the causal direction [Mooij et al., 2016, Tagasovska et al., 2020]. The simple heuristic confidence [Mooij et al., 2016] is adopted here. For instance, for the proposed OCD, we define the confidence of $X \to Y$ to be $C_{X \to Y} = \text{BIC}(Y \to X|\boldsymbol{x}) - \text{BIC}(X \to Y|\boldsymbol{x})$.

Results. In Table 2, we summarize the ACC, AUC, and CPU times. For OCD and HCR, the average metrics over $L = 10, \ldots, 20$ as well as their standard errors are reported. The proposed OCD is highly competitive in all metrics. OCD has the second highest ACC and AUC, and is fast; it completes the analysis of 99 datasets in 36 seconds. Only IGCI, CAM, and LiNGAM are faster but they have worse ACC and AUC than OCD. SLOPE has slightly higher ACC and AUC than OCD. However, SLOPE is about 1 or 2 orders of magnitude slower than OCD and relatively sensitive to small added noise (see the additional experiments that investigate the "Sensitivity to Small Added Noise" in the Supplementary Materials). Finally, the small standard errors of the performance metrics of OCD indicate its relative robustness with respect to the number L of levels of discretization for the considered datasets and range.

Table 2: CEP data. Metrics of OCD and HCR are averaged over different values of $L = 10, \ldots, 20$ with standard errors given within the parentheses.

	OCD	HCR	bQCD	CAM
ACC	0.73 (0.01)	0.44 (0.02)	0.70	0.58
AUC	0.76 (0.00)	0.56 (0.02)	0.72	0.58
CPU	36s (1.7s)	12m (2.2m)	7m	11s
	IGCI	SLOPE	LiNGAM	RESIT
ACC	0.66	0.76	0.42	0.53
AUC	0.51	0.84	0.59	0.56
CPU	1s	24m	3s	12h

6.4 SINGLE-CELL RNA-SEQUENCING DATA

We further validate the proposed OCD with a publicly available single-cell RNA-sequencing (scRNA-seq) dataset of $2,717$ murine embryonic stem cells [Klein et al., 2015]. We obtain a list of literature-curated pairs of transcription factor (X) and its target (Y) from the TRRUST database [Han et al., 2018], which provides biological ground truth of the casual relationships, namely $X \to Y$. We then extract the corresponding genes from the scRNA-seq dataset. Removing genes with more than 90% zeros (these genes have very low statistical variability), we retained 6701 pairs for causal validation which still have 62% zeros. The zeros in scRNA-seq data are either (a) true biological zero counts or (b) small counts that are too low to detect. In either case, they can be regarded as "low expression". We compare OCD with the best performing methods in Section 6.3, bQCD and SLOPE, as well as the closest competitor HCR. We are not able to generate results (runtime errors) from CAM, LiNGAM, and RESIT possibly because of the large percentages of zeros. To apply OCD and HCR, we trichotomize the data at 0 and the median of the non-zero expression (i.e., "low", "average", and "high" expression). ACC and CPU time are reported in Table 3. OCD is the best and is the only method that is better than random guess (p-value = 10^{-75}, binomial test with $H_0 : p = 0.5$ vs $H_a : p > 0.5$) for this dataset possibly because of its highly non-standard distribution due to zero-inflation. Therefore, although discretizing continuous or count data may lose information, it often improves the robustness by not having to impose a particular distributional assumption on the raw data.

Table 3: Single-cell RNA-seq data.

	OCD	HCR	bQCD	SLOPE
ACC	0.61	0.36	0.45	0.50
CPU	19m	22m	3.4h	2h

7 CONCLUSION

There are several limitations of the current work, which we plan to address in our future work. First, the current score-and-search algorithm outputs a point estimate of the causal graph with no uncertainty quantification. We plan to develop a fully Bayesian approach by assigning sparse priors (i.e., spike-and-slab priors on β's) and carrying out posterior inference via the Markov chain Monte Carlo. Second, we have empirically assessed the identifiability of the proposed OCD for multivariate data and for bivariate data with unmeasured confounders. The identifiability theory for multivariate categorical data or bivariate categorical data with unmeasured confounders is in general lacking in the causal discovery literature. Third, we have not explicitly addressed the problem of choosing the number L of categories in data discretization. We picked $L = 3$ for genomic data by convention and assessed its robustness up to $L = 10$. For non-genomic data, there is no obvious/universal choice of L. Instead of picking a specific L, we have tested the proposed OCD in a range of values. In the future, we plan to propose data-driven ways (e.g., via BIC) to objectively choose L.

References

Alan Agresti. *Categorical Data Analysis*, volume 482. John Wiley & Sons, 2003.

Patrick Blöbaum, Dominik Janzing, Takashi Washio, Shohei Shimizu, and Bernhard Schölkopf. Cause-effect inference by comparing regression errors. In *International Conference on Artificial Intelligence and Statistics*, pages 900–909, 2018.

Peter Bühlmann, Jonas Peters, Jan Ernest, et al. Cam: Causal additive models, high-dimensional order search and penalized regression. *The Annals of Statistics*, 42(6):2526–2556, 2014.

Ruichu Cai, Jie Qiao, Kun Zhang, Zhenjie Zhang, and Zhifeng Hao. Causal discovery from discrete data using hidden compact representation. *Advances in Neural Information Processing Systems*, 2018:2666, 2018.

Zhitang Chen, Kun Zhang, Laiwan Chan, and Bernhard Schölkopf. Causal discovery via reproducing kernel Hilbert space embeddings. *Neural Computation*, 26(7): 1484–1517, 2014.

David Maxwell Chickering. Optimal structure identification with greedy search. *Journal of Machine Learning Research*, 3(Nov):507–554, 2002.

Junsouk Choi, Robert Chapkin, and Yang Ni. Bayesian causal structural learning with zero-inflated Poisson Bayesian networks. In *Advances in Neural Information Processing Systems 33*, 2020.

Spencer Compton, Murat Kocaoglu, Kristjan Greenewald, and Dmitriy Katz. Entropic causal inference: Identifiability and finite sample results. In *Advances in Neural Information Processing Systems*, volume 33, pages 14772–14782. Curran Associates, Inc., 2020.

Ruifei Cui, Perry Groot, Moritz Schauer, and Tom Heskes. Learning the causal structure of copula models with latent variables. In *Proceedings of the Thirty-Fourth Conference on Uncertainty in Artificial Intelligence*, page 188–197, 2018.

Nir Friedman and Daphne Koller. Being Bayesian about network structure. A Bayesian approach to structure discovery in Bayesian networks. *Machine Learning*, 50(1-2): 95–125, 2003.

Heonjong Han et al. TRRUST v2: an expanded reference database of human and mouse transcriptional regulatory interactions. *Nucleic Acids Research*, 46(D1): D380–D386, 2018.

David Heckerman, Dan Geiger, and David M Chickering. Learning Bayesian networks: The combination of knowledge and statistical data. *Machine Learning*, 20(3):197–243, 1995.

Daniel Hernandez-Lobato, Pablo Morales-Mombiela, David Lopez-Paz, and Alberto Suarez. Non-linear causal inference using Gaussianity measures. *The Journal of Machine Learning Research*, 17(1):939–977, 2016.

Patrik O Hoyer, Dominik Janzing, Joris M Mooij, Jonas Peters, and Bernhard Schölkopf. Nonlinear causal discovery with additive noise models. In *Advances in Neural Information Processing Systems*, pages 689–696, 2009.

Dominik Janzing, Joris Mooij, Kun Zhang, Jan Lemeire, Jakob Zscheischler, Povilas Daniušis, Bastian Steudel, and Bernhard Schölkopf. Information-geometric approach to inferring causal directions. *Artificial Intelligence*, 182:1–31, 2012.

Allon M Klein et al. Droplet barcoding for single-cell transcriptomics applied to embryonic stem cells. *Cell*, 161(5):1187–1201, 2015.

Furui Liu and Laiwan Chan. Causal inference on discrete data via estimating distance correlations. *Neural Computation*, 28(5):801–814, 2016.

Alexander Marx and Jilles Vreeken. Telling cause from effect using MDL-based local and global regression. In *2017 IEEE International Conference on Data Mining (ICDM)*, pages 307–316. IEEE, 2017.

Alexander Marx and Jilles Vreeken. Identifiability of cause and effect using regularized regression. In *Proceedings of the 25th ACM SIGKDD International Conference on Knowledge Discovery & Data Mining*, pages 852–861, 2019.

Joris M Mooij, Oliver Stegle, Dominik Janzing, Kun Zhang, and Bernhard Schölkopf. Probabilistic latent variable models for distinguishing between cause and effect. In *Advances in Neural Information Processing Systems*, pages 1687–1695, 2010.

Joris M Mooij, Jonas Peters, Dominik Janzing, Jakob Zscheischler, and Bernhard Schölkopf. Distinguishing cause from effect using observational data: methods and benchmarks. *The Journal of Machine Learning Research*, 17(1):1103–1204, 2016.

Gunwoong Park and Hyewon Park. Identifiability of generalized hypergeometric distribution (GHD) directed acyclic graphical models. In *The 22nd International Conference on Artificial Intelligence and Statistics*, pages 158–166, 2019.

Gunwoong Park and Garvesh Raskutti. Learning large-scale Poisson DAG models based on overdispersion scoring. In *Advances in Neural Information Processing Systems*, pages 631–639, 2015.

Giovanni Parmigiani et al. A statistical framework for expression-based molecular classification in cancer. *Journal of the Royal Statistical Society: Series B*, 64(4):717–736, 2002.

Judea Pearl. *Causality: Models, Reasoning and Inference*. Cambridge University Press, USA, 2nd edition, 2009. ISBN 052189560X.

Dana Pe'er. Bayesian network analysis of signaling networks: a primer. *Science's STKE*, 2005(281):pl4–pl4, 2005.

Jonas Peters and Peter Bühlmann. Identifiability of Gaussian structural equation models with equal error variances. *Biometrika*, 101(1):219–228, 2014.

Jonas Peters and Peter Bühlmann. Structural intervention distance for evaluating causal graphs. *Neural Computation*, 27(3):771–799, 2015.

Jonas Peters, Dominik Janzing, and Bernhard Schölkopf. Identifying cause and effect on discrete data using additive noise models. In *Proceedings of the Thirteenth International Conference on Artificial Intelligence and Statistics*, pages 597–604, 2010.

Jonas Peters, Joris M Mooij, Dominik Janzing, and Bernhard Schölkopf. Causal discovery with continuous additive noise models. *The Journal of Machine Learning Research*, 15(1):2009–2053, 2014.

Joseph Ramsey, Jiji Zhang, and Peter L Spirtes. Adjacency-faithfulness and conservative causal inference. *arXiv preprint arXiv:1206.6843*, 2012.

Karen Sachs, Omar Perez, Dana Pe'er, Douglas A Lauffenburger, and Garry P Nolan. Causal protein-signaling networks derived from multiparameter single-cell data. *Science*, 308(5721):523–529, 2005.

Marco Scutari and Jean-Baptiste Denis. *Bayesian Networks: with Examples in R*. CRC press, 2014.

Marco Scutari, Claudia Vitolo, and Allan Tucker. Learning Bayesian networks from big data with greedy search: Computational complexity and efficient implementation. *Statistics and Computing*, 29(5):1095–1108, 2019.

Andrew J Sedgewick et al. Mixed graphical models for integrative causal analysis with application to chronic lung disease diagnosis and prognosis. *Bioinformatics*, 35 (7):1204–1212, 2019.

Eleni Sgouritsa, Dominik Janzing, Philipp Hennig, and Bernhard Schölkopf. Inference of cause and effect with unsupervised inverse regression. In *Artificial Intelligence and Statistics*, pages 847–855, 2015.

Xinpeng Shen, Sisi Ma, Prashanthi Vemuri, and Gyorgy Simon. Challenges and opportunities with causal discovery algorithms: Application to Alzheimer's pathophysiology. *Scientific Reports*, 10(1):1–12, 2020.

Shohei Shimizu, Patrik O Hoyer, Aapo Hyvärinen, and Antti Kerminen. A linear non-Gaussian acyclic model for causal discovery. *Journal of Machine Learning Research*, 7(Oct):2003–2030, 2006.

Peter Spirtes and Kun Zhang. Causal discovery and inference: Concepts and recent methodological advances. *Applied Informatics*, 3(1):3, 2016.

Peter Spirtes, Clark N Glymour, Richard Scheines, and David Heckerman. *Causation, Prediction, and Search*. MIT press, 2000.

Mark Steyvers, Joshua B Tenenbaum, Eric-Jan Wagenmakers, and Ben Blum. Inferring causal networks from observations and interventions. *Cognitive Science*, 27(3): 453–489, 2003.

Joe Suzuki, Takanori Inazumi, Takashi Washio, and Shohei Shimizu. Identifiability of an integer modular acyclic additive noise model and its causal structure discovery. *arXiv preprint arXiv:1401.5625*, 2014.

Natasa Tagasovska, Valérie Chavez-Demoulin, and Thibault Vatter. Distinguishing cause from effect using quantiles: Bivariate quantile causal discovery. In *International Conference on Machine Learning*, pages 9311–9323. PMLR, 2020.

Michail Tsagris, Giorgos Borboudakis, Vincenzo Lagani, and Ioannis Tsamardinos. Constraint-based causal discovery with mixed data. *International Journal of Data Science and Analytics*, 6(1):19–30, 2018.

Ioannis Tsamardinos, Constantin F Aliferis, Alexander R Statnikov, and Er Statnikov. Algorithms for large scale Markov blanket discovery. In *FLAIRS Conference*, volume 2, pages 376–380, 2003.

Wenjuan Wei, Lu Feng, and Chunchen Liu. Mixed causal structure discovery with application to prescriptive pricing. In *Proceedings of the 27th International Joint Conference on Artificial Intelligence*, pages 5126–5134, 2018.

Kun Zhang and Aapo Hyvärinen. On the identifiability of the post-nonlinear causal model. In *Proceedings of the Twenty-Fifth Conference on Uncertainty in Artificial Intelligence*, UAI '09, page 647–655, Arlington, Virginia, USA, 2009. AUAI Press. ISBN 9780974903958.

Ordinal Causal Discovery: Supplementary Materials

1 Proof of Theorem 1

We need the notion of *real analytic function.*

Definition (Real Analytic Function) *A real function is said to be analytic if it is infinitely differentiable and matches its Taylor series in a neighborhood of every point.*

Suppose $X \in \{1, \ldots, S\}$ and $Y \in \{1, \ldots, L\}$. Consider two competing causal models $p_{X\to Y}(X, Y|\boldsymbol{\pi}, \boldsymbol{\beta}, \boldsymbol{\gamma})$ and $p_{Y\to X}(Y, X|\boldsymbol{\rho}, \boldsymbol{\alpha}, \boldsymbol{\eta})$. We will show that these two causal models are in general not equivalent, i.e., $P_{X\to Y}(X = s, Y = \ell|\boldsymbol{\pi}, \boldsymbol{\beta}, \boldsymbol{\gamma}) \neq P_{Y\to X}(X = s, Y = \ell|\boldsymbol{\rho}, \boldsymbol{\alpha}, \boldsymbol{\eta})$ for some $s \in \{1, \ldots, S\}$ and $\ell \in \{1, \ldots, L\}$, where $S, L \geq 2$ and $\max\{S, L\} \geq 3$. Without loss of generality, assume $S \geq 3$. We prove it by contradiction. Suppose for any $s \in \{1, \ldots, S\}$ and $\ell \in \{1, \ldots, L\}$,

$$P_{X\to Y}(X = s, Y = \ell|\boldsymbol{\pi}, \boldsymbol{\beta}, \boldsymbol{\gamma}) = P_{Y\to X}(X = s, Y = \ell|\boldsymbol{\rho}, \boldsymbol{\alpha}, \boldsymbol{\eta}). \tag{1}$$

The left-hand side of (1) is given by

$$\begin{aligned} P_{X\to Y}(X = s, Y = \ell|\boldsymbol{\pi}, \boldsymbol{\beta}, \boldsymbol{\gamma}) &= P_{X\to Y}(Y = \ell|X = s, \boldsymbol{\beta}, \boldsymbol{\gamma})P_{X\to Y}(X = s|\boldsymbol{\pi}) \\ &= [P_{X\to Y}(Y \leq \ell|X = s, \boldsymbol{\beta}, \boldsymbol{\gamma}) - P_{X\to Y}(Y \leq \ell - 1|X = s, \boldsymbol{\beta}, \boldsymbol{\gamma})]P_{X\to Y}(X = s|\boldsymbol{\pi}) \\ &= [F(\gamma_\ell - \beta_s) - F(\gamma_{\ell-1} - \beta_s)]\pi_s, \end{aligned}$$

where $F(x)$ is the logistic $F(x) = \frac{e^x}{1+e^x}$ or the probit $F(x) = \Phi(x)$ link function where $\Phi(x)$ is the standard normal cumulative distribution function. Similarly, the right-hand side of (1) is given by

$$P_{Y\to X}(X = s, Y = \ell|\boldsymbol{\rho}, \boldsymbol{\alpha}, \boldsymbol{\eta}) = P_{Y\to X}(X = s|Y = \ell, \boldsymbol{\alpha}, \boldsymbol{\eta})P_{Y\to X}(Y = \ell|\boldsymbol{\rho}) = [F(\eta_s - \alpha_\ell) - F(\eta_{s-1} - \alpha_\ell)]\rho_\ell.$$

Therefore, (1) leads to

$$[F(\gamma_\ell - \beta_s) - F(\gamma_{\ell-1} - \beta_s)]\pi_s = [F(\eta_s - \alpha_\ell) - F(\eta_{s-1} - \alpha_\ell)]\rho_\ell \tag{2}$$

Note that the right-hand side of (2) is a telescoping series in s. Hence, summing up both sides of (2) over s from 1 to S, we have

$$\begin{aligned} \sum_{s=1}^{S}[F(\gamma_\ell - \beta_s) - F(\gamma_{\ell-1} - \beta_s)]\pi_s &= [F(\eta_S - \alpha_\ell) - F(\eta_0 - \alpha_\ell)]\rho_\ell \\ &= \rho_\ell. \end{aligned} \tag{3}$$

The last equation is because $\eta_S = \infty$ and $\eta_0 = -\infty$ and hence $F(\eta_S - \alpha_\ell) = 1$ and $F(\eta_0 - \alpha_\ell) = 0$. Plug (3) into (2),

$$[F(\gamma_\ell - \beta_s) - F(\gamma_{\ell-1} - \beta_s)]\pi_s = [F(\eta_s - \alpha_\ell) - F(\eta_{s-1} - \alpha_\ell)]\sum_{s=1}^{S}[F(\gamma_\ell - \beta_s) - F(\gamma_{\ell-1} - \beta_s)]\pi_s$$

and hence

$$\frac{[F(\gamma_\ell - \beta_s) - F(\gamma_{\ell-1} - \beta_s)]\pi_s}{\sum_{s=1}^{S}[F(\gamma_\ell - \beta_s) - F(\gamma_{\ell-1} - \beta_s)]\pi_s} = F(\eta_s - \alpha_\ell) - F(\eta_{s-1} - \alpha_\ell) \tag{4}$$

Now, consider $s = 1$ in (4) and note $\eta_0 = -\infty$ and $\eta_1 = 0$,

$$\begin{aligned}\frac{[F(\gamma_\ell - \beta_1) - F(\gamma_{\ell-1} - \beta_1)]\pi_1}{\sum_{s=1}^{S}[F(\gamma_\ell - \beta_s) - F(\gamma_{\ell-1} - \beta_s)]\pi_s} &= F(\eta_1 - \alpha_\ell) - F(\eta_0 - \alpha_\ell) \\ &= F(-\alpha_\ell).\end{aligned}$$

Therefore,

$$\alpha_\ell = -F^{-1}\left\{\frac{[F(\gamma_\ell - \beta_1) - F(\gamma_{\ell-1} - \beta_1)]\pi_1}{\sum_{s=1}^{S}[F(\gamma_\ell - \beta_s) - F(\gamma_{\ell-1} - \beta_s)]\pi_s}\right\} \tag{5}$$

Sequentially plug (5) into (4) for $s^* = 2, \ldots, S-1$ (note that one can at least plug in once for $s^* = 2$ because $S \geq 3$),

$$\eta_{s^*} = F^{-1}\left\{\frac{\sum_{s=1}^{s^*}[F(\gamma_\ell - \beta_s) - F(\gamma_{\ell-1} - \beta_s)]\pi_s}{\sum_{s=1}^{S}[F(\gamma_\ell - \beta_s) - F(\gamma_{\ell-1} - \beta_s)]\pi_s}\right\} - F^{-1}\left\{\frac{[F(\gamma_\ell - \beta_1) - F(\gamma_{\ell-1} - \beta_1)]\pi_1}{\sum_{s=1}^{S}[F(\gamma_\ell - \beta_s) - F(\gamma_{\ell-1} - \beta_s)]\pi_s}\right\}, \tag{6}$$

Because the left-hand side of (6) is independent of ℓ whereas the right-hand side of (6) depends on ℓ, we have,

$$\begin{aligned}&F^{-1}\left\{\frac{\sum_{s=1}^{s^*}[F(\gamma_\ell - \beta_s) - F(\gamma_{\ell-1} - \beta_s)]\pi_s}{\sum_{s=1}^{S}[F(\gamma_\ell - \beta_s) - F(\gamma_{\ell-1} - \beta_s)]\pi_s}\right\} - F^{-1}\left\{\frac{[F(\gamma_\ell - \beta_1) - F(\gamma_{\ell-1} - \beta_1)]\pi_1}{\sum_{s=1}^{S}[F(\gamma_\ell - \beta_s) - F(\gamma_{\ell-1} - \beta_s)]\pi_s}\right\} \\ -F^{-1}&\left\{\frac{\sum_{s=1}^{s^*}[F(\gamma_{\ell^*} - \beta_s) - F(\gamma_{\ell^*-1} - \beta_s)]\pi_s}{\sum_{s=1}^{S}[F(\gamma_{\ell^*} - \beta_s) - F(\gamma_{\ell^*-1} - \beta_s)]\pi_s}\right\} + F^{-1}\left\{\frac{[F(\gamma_{\ell^*} - \beta_1) - F(\gamma_{\ell^*-1} - \beta_1)]\pi_1}{\sum_{s=1}^{S}[F(\gamma_{\ell^*} - \beta_s) - F(\gamma_{\ell^*-1} - \beta_s)]\pi_s}\right\} = 0,\end{aligned} \tag{7}$$

for any $\ell, \ell^* \in \{1, \ldots, L\}$ and $\ell \neq \ell^*$ (note that one can always find $\ell \neq \ell^*$ because $L \geq 2$). The link function F is an analytic function: (i) the logistic link $F(x) = \frac{e^x}{1+e^x}$ is a composition of elementary functions and hence is analytic; and (ii) the probit link $F(x) = \Phi(x)$ is analytic because the error function erf() is analytic. Since $F'(x)$ is nowhere zero in either case, $F^{-1}(x)$ is analytic. Since the left-hand side of (7) is a composition of F, F^{-1}, sums, products, and reciprocals of $r_\ell, r_{\ell^*}, r_{\ell-1}, r_{\ell^*-1}, b_1, \ldots, b_S, \pi_1, \ldots, \pi_S$, it is an analytic function (Krantz and Parks, 2002) and therefore its zero set must have Lebesgue measure zero (Mityagin, 2015). In summary, we have proven that the two causal models are not equivalent for almost all $(\boldsymbol{\pi}, \boldsymbol{\beta}, \boldsymbol{\gamma})$ with respect to the Lebesgue measure. Note that although our proof is for logistic or probit link, it is generalizable to other link functions as long as they are analytic functions and their derivatives are nowhere zero.

2 Additional Experiment Results

2.1 Synthetic Data

Number of Categories $L = 3$ We investigate scenarios where the number of categories $L = 3$. The data are generated as in the main text ($n = 500, p = 10$) except that the number of categories is now set to $L = 3$. Six scenarios with different levels of signal strength are considered, $\sigma = 0.25, 0.5, 0.75, 1, 1.25, 1.5$. We report the SHD of OCD, BIC+, BIC, and BDe in Table 1, which shows that OCD significantly outperforms competing methods.

Higher-Dimensional Synthetic Data As shown in Figure 1, for all tested signal strength $\sigma \in \{0.25, 0.5, 0.75, 1\}$ and number of nodes $p = 10, \ldots, 100$, SHD and SID of OCD are uniformly better than the competing methods and in general, OCD is quite stable as p increases when the signal strength is at least moderate $\sigma \geq 0.5$ whereas the competing methods quickly deteriorate with p regardless of the signal strength.

The CPU times of OCD in the synthetic data are shown in Figure 2, which appear to scale linearly in n and L, and quadratically in p.

Synthetic Data with Denser Graphs We consider a scenario with $n = 500$ observations, $p = 50$ nodes, and $L = 5$ categories. We randomly generate graphs with 25, 50, and 100 edges (Figure 3). We report the Structural hamming distance (SHD) between the true graph and the estimated graphs from OCD, BIC+, BIC, and BDe in Table 2. We find very minor decrease in performance of OCD whereas the competing methods perform substantially worse and deteriorate much faster.

	Signal Strength σ					
	0.25	0.5	0.75	1	1.25	1.5
OCD	5.2	1.6	1	0.8	0.2	0.2
BIC+	6.4	5	3.6	3.8	3.8	3.6
BIC	7	5.8	4.6	4	3.2	3.8
BDe	7	6.8	6.2	5.2	5	4.6

Table 1: Structural hamming distance between the true graph and the estimated graphs from OCD, BIC+, BIC, and BDe. The data are generated as in the main text with different levels of signal strength except that the number of categories is set to $L = 3$.

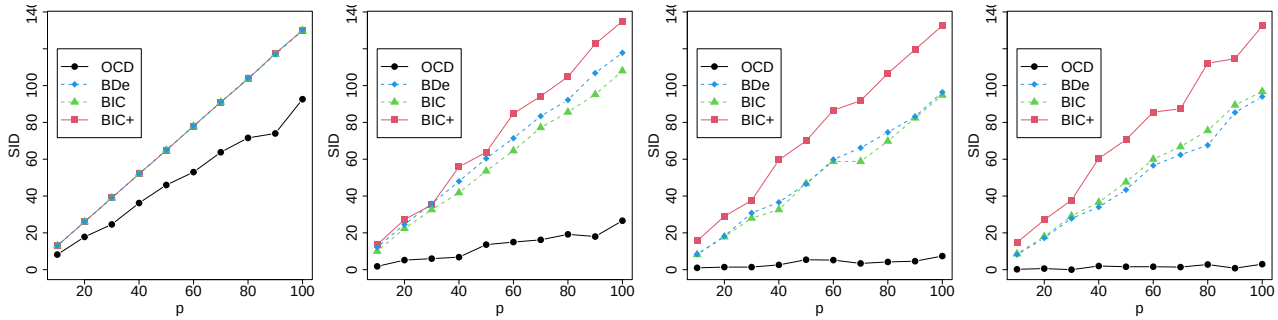

(a) SID in p ($\sigma = 0.25$) (b) SID in p ($\sigma = 0.5$) (c) SID in p ($\sigma = 0.75$) (d) SID in p ($\sigma = 1$)

Figure 1: SID for OCD, BDe, BIC, and BIC+ as functions of p in the synthetic ordinal data with the sample size fixed at $n = 500$ and different signal strength $\sigma \in \{0.25, 0.5, 0.75, 1\}$.

2.2 Real Data

Sensitivity to Small Added Noise to CEP Data Following the idea in Mooij et al. 2016, we test the sensitivity of the best performing causal discovery methods (OCD with $L = 15$, SLOPE, and bQCD) to small added noises. Specifically, we add independent centered Gaussian noise to X and Y with standard deviation $\tau \in \{10^{-8}, 10^{-7}, \ldots, 10^{-1}\}$. We repeat the simulation of noises 5 times under each noise level and the average ACC and AUC are shown in Figure 4. All methods have stable performance for $\tau = 10^{-8} - 10^{-5}$. The performance of SLOPE starts deteriorating at $\tau = 10^{-4}$ whereas OCD and bQCD are much more robust (significant drop in ACC at $\tau = 10^{-1}$). The robustness of OCD is expected because small added noise will not significantly affect data discretization.

References

Krantz, S. G. and Parks, H. R. (2002). *A primer of real analytic functions*. Springer Science & Business Media.

Mityagin, B. (2015). The zero set of a real analytic function. *arXiv preprint arXiv:1512.07276*.

Mooij, J. M., Peters, J., Janzing, D., Zscheischler, J., and Schölkopf, B. (2016). Distinguishing cause from effect using observational data: methods and benchmarks. *The Journal of Machine Learning Research*, 17(1):1103–1204.

	# of Edges		
	25	50	100
OCD	0	0	1
BIC+	13	-	-
BIC	25	48	92
BDe	23	40	75

Table 2: Structural hamming distance between the true graph and the estimated graphs from OCD, BIC+, BIC, and BDe. The true graphs are generated randomly with 25, 50, and 100 edges. BIC+ is not applicable for 50 and 100 edges as it takes 150GB of memory.

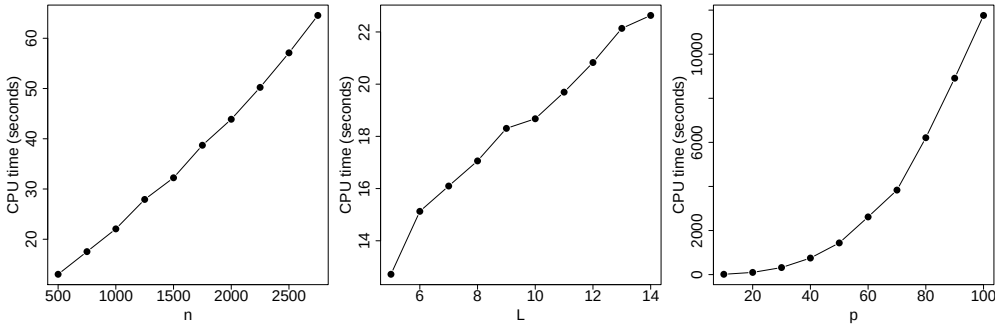

(a) CPU time in n (b) CPU time in L (c) CPU time in p

Figure 2: CPU times of OCD as functions of n, L, and p in the synthetic ordinal data.

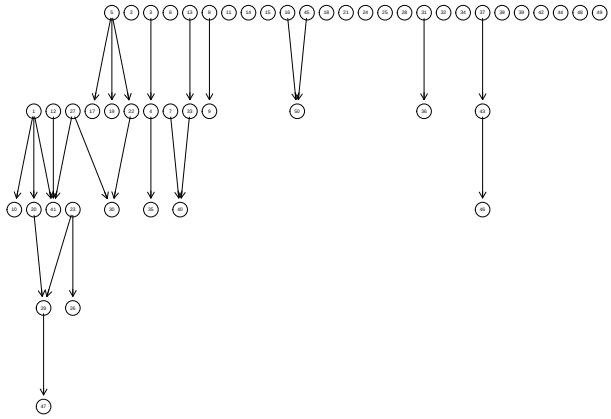

(a) 25 edges

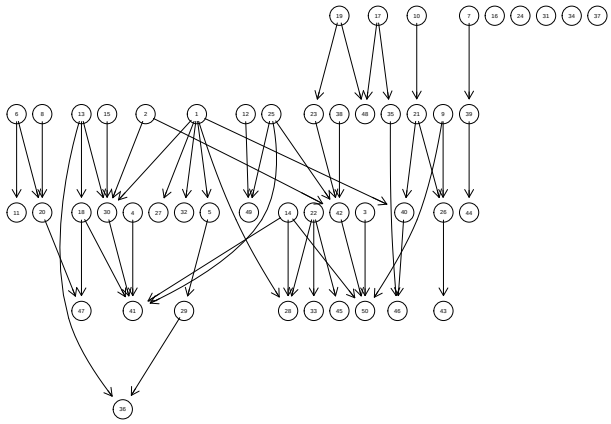

(b) 50 edges

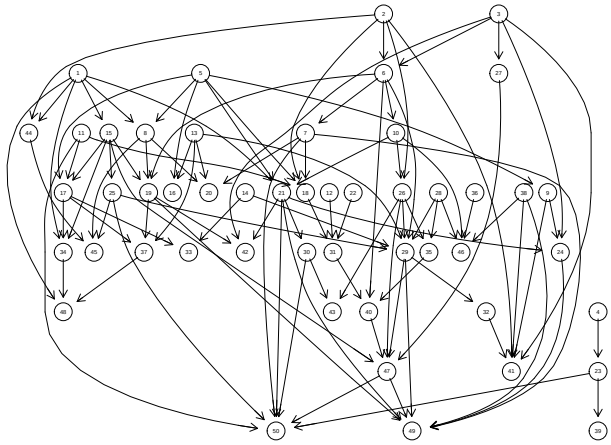

(c) 100 edges

Figure 3: Simulation truth of denser graphs.

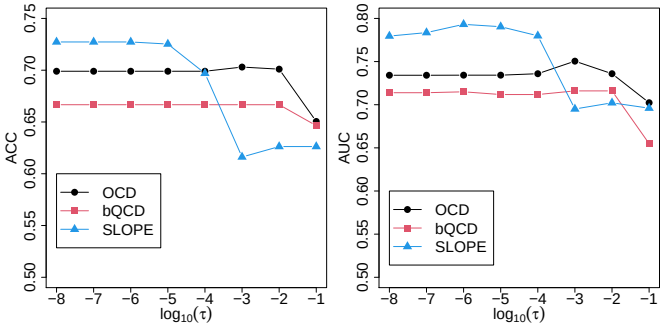

(a) ACC (b) AUC

Figure 4: Sensitivity to small added noise for the CEP data.